PROCEEDINGS, 50th Workshop on Geothermal Reservoir Engineering
Stanford University, Stanford, California, February 10-12, 2025
SGP-TR-229

Thermodynamic Analysis of Liptov Basin (Slovakia) Using Geostatistical Uncertainty Modelling

Ladislav Vizi, Branislav Fričovský, Klement Fordinál, Radovan Černák

State Geological Institute of Dionýz Štúr, Mlynská dolina 1, 81704 Bratislava, Slovakia

ladislav.vizi@geology.sk

Keywords: geostatistical modelling, numerical model, post-processing, cut-off, thermodynamical parameters

ABSTRACT

Geothermal energy in Slovakia has been under systematic research since the second half of the last century. Nowadays, more than thirty prospective geothermal fields in Slovakia have been identified and described. The Liptov basin is considered one of the most promising geothermal fields due to a set of local hydrogeothermal structures, which opens a space for different uses of geothermal waters. From the point of view of thermodynamic quality and reservoir potential, modelling of the reservoir parameters aims to provide information about the most efficient way to use geothermal energy resources, based on a balance between the purpose of a future use and the reservoir's parameters. Utilising existing temperature and initial thermodynamic quantities, such as enthalpy and exergy, defining on regularly spaced calculation points, which are directly connected to the results of the stationary geothermic models, we built a set of 3D stochastic models using geostatistical simulation. The turning band method of the spatial simulation was used due to evident non-stationarity behaviour in a vertical direction as the consequence of a positive depth-temperature relationship. The geostatistical simulations aim to create multiple realisations of the studied thermodynamic variables to create a numerical model. Subsequent assessments and classifications of the thermodynamic quality of energy sources regarding the processing of the numerical models for the defined thresholds (cut-offs) to obtain the spatial distributions of the studied thermodynamic variables and probabilities above the cut-offs. The processed results of the spatial modelling were applied for the typology of both reservoir units and the individual structures, concerning the local specifics such as urbanisation, industry, agriculture or public services. The results provide support for decision-making processes in national and local administration as well as for the potential private investors during their project preparation and the investment consideration or minimizing the failure risks due to the project intention.

1. INTRODUCTION

Occurrence of thermal and mineral waters in Slovakia is well known for centuries, however, first systematic research dates to 1920's. Oil crisis prompted intense geophysical prospection on oil and gas resources during 1960 – 1970, which resulted in promising geothermal potential in the country. Systematic research and development of the geothermal energy dates back to the 70's of the last Century and progressively increases a number of geothermal installations in a direct-use. Nowadays, with 31 geothermal water bodies, covering roughly 40 % of Slovakia (Fričovský et al., 2024), the geothermal energy appears to be a significant source of energy of the country. This is also the case of the Liptov basin.

Regional geological structure of the Liptov basin corresponds to vertical architecture typical for Western Carpathian's Tertiary intermountain depressions with the crystalline buried deep beneath Mesozoic carbonates and Eocene – Oligocene sedimentary succession, with topmost Quaternary formations. Five principal tectonic units are identified within the Liptov basin: Tatricum Crystalline, Tatricum Envelope Unit, Krížna Nappe, Choč Nappe and the Inner Western Carpathian Paleogene (IWCP), all in various, tectonic (thrust) or transgressive (discordant) relations. The Liptov basin geothermal field distinguishes several flow systems within Mid Triassic carbonates of the Choc and Krížna Nappes (Figure 1). The shallow geothermal reservoir (RES1) forms a system composing of the Choc Nappe Mid – Late Triassic carbonates (dolomites prevail) in hydraulic connection with the IWCP formations, all covered by Quaternary (upper insulator – ISO1).The deep geothermal reservoir (RES2) in Mid Triassic carbonates of the Krížna Nappe forms a solid body through the entire system. Above, clayey dolomites, clays and shales of the Late Triassic occur beneath duplexed Jurassic – Mid Cretaceous succession including marlstones, claystones and their transient types; all representing lower insulator (ISO2) (Remšík et al., 1998; Vandrová et al., 2009). Where the slag of the Choc Nappe is missing, the Krížna Nappe forms a pre-Paleogene basement.

Geothermal reservoirs, like many other natural systems, are typical by their incomplete, discontinuous and sparse, irregularly distributed information that are heterogeneous and highly variable within a domain under study. Similarly to the mineral deposits, petroleum reservoirs or contaminated sites, geothermal reservoirs can only be known or measured in an incomplete and fractional manner. Unfortunately, in a stage of a reservoir management, dynamic simulation, decision making or risk analysis that used to study and predict the behaviour of a geothermal system require continuous parameters at the places where they have never been or cannot be measured. Geothermal reservoirs and their internal processes originate and evolve partially in a random way (Arriaga and Samaniego, 1998). Since randomness is just another term for our lack of knowledge, it means that it is impossible to perform exact prediction about unknown values. It calls for a spatial modelling of the unknown values at unsampled positions.

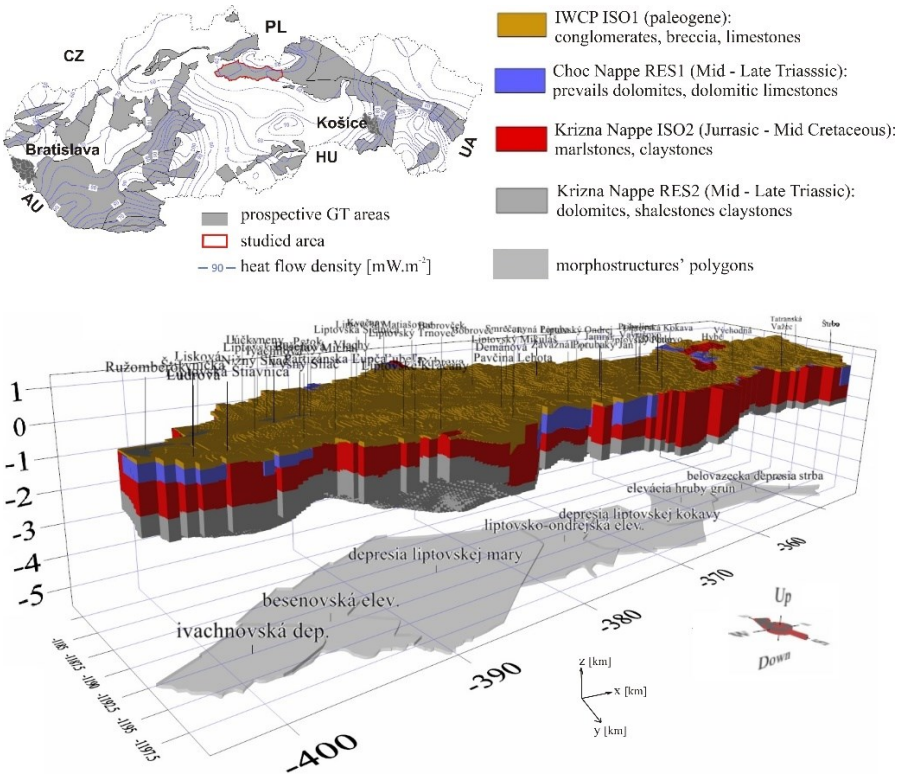

Figure 1: Liptov basin location and basic geological model.

In Slovakia, it is common practise to use some deterministic predictions to model a natural phenomenon in form of a spatial distribution of a variable under study. The goal of using deterministic interpolations is very simple: to meet own conceptual model, virtually created in a head on the knowledge base. As stated in Bond and Gibbs (2015), humans are very good at applying conceptual analogues to data, and if our analogues do not fit the data, our brains will try and fit what is there to our concepts (preconceptions and notions). Unfortunately, "to fit what is there to our concept" often means to use default parameters of the very first interpolation method within an available 2D or 3D software without performing some adjustment of the interpolation parameters to the data. This often leads to unacceptable results such as estimating negative values of a strictly positive random variable or, what is much worse, inserting new synthetic data. Thereafter, a set of visualised (and corrected) results of the selected data interpolation in different depths are used to delineate the subareas above a selected threshold in a strong believe that the single, final result is the only correct and singular one. The main drawback of such approach lies in fact that colourful result is not singular one at all, but rather one of many possible. As Clayton Deutsh, a well-known authority in geostatistics, highlights "we are not interested in pretty pictures" (Deutsh, 2002).

Presented case study deals with a different approach. The general purpose of the paper is to present applications of stochastic simulations to assess spatial uncertainty of selected thermodynamical (hereafter TD) parameters and spatially delimit the geothermal reservoir above a set of threshold values (cut-offs). Combination of occurrence TD parameter values above cut-offs and probability of that occurrence leads to the selections of a potential use the geothermal resources for individual hydrogeothermal structures within Liptov basin. We present some basic geostatistics concepts and preliminary results based on them because it is underutilised in Slovak geothermal sector. The presented case study is only one of few processed by the authors (Fričovský et al., 2019, Vizi et al. 2024). The intension is not to provide a detail review of available geostatistical techniques, nor to compare them. The aim is rather to summarise the used workflow and results in hope that those concerned with routine manipulation of available data, predominantly by applying traditional statistical methods, will be encouraged to take advantage of the benefits available from geostatistics.

2. THERORY

2.2 Non-stationary modelling and estimation

Geostatistics is a rapidly evolving scientific branch of applied statistics and mathematics that studies the spatial-temporal phenomena and thus extends the concept of traditional statistical methods of data processing in a spatial form. It was originally developed by George Matheron of Centre de Morphologie Mathématique in France for solving the problems of the ore reserve estimation in the mining industry but it is nowadays very popular not only in geology but also in many other areas of the natural science. Spatial data, in the framework of geosciences, exhibit some degree of spatial correlation, which is a function of the distance – the greater the distance between samples, the lower the similarity between the data, but on the contrary, the higher is their variability (Matheron, 1963).

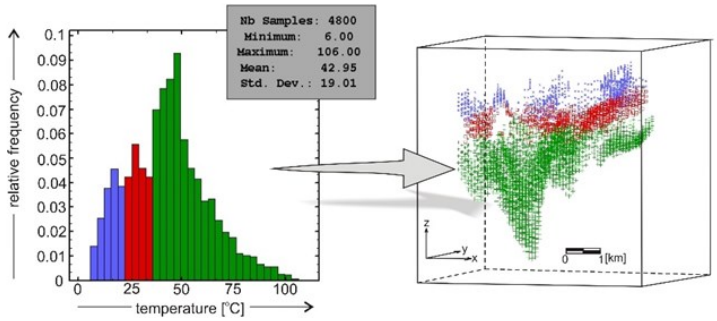

Figure 2: Example of multimodal histogram showing subpopulations of temperature as a function of depth.

Geostatistics provides a wide variety of tools to quantify and model the degree of spatial similarity and spatial variability. The aim of geostatistical methods for modelling of spatial variability is a random variable Z distributed in space and/or time. In geostatistical applications, a random variable is a function of spatial coordinates at any point of the studied area, in which each point $\mathbf{u}$ is determined by geographic (and/or time) coordinates in one, two or three-dimensional space; $\mathbf{u}$ = (X, Y, Z). Set of such random variables at each point $\mathbf{u}$ of the studied domain D represents a random function $Z(\mathbf{u})$. One realisation of a random function, or one realisation of each random variable in the space, consists of a set of values $z(\mathbf{u})$ called a regionalised variable (Matheron, 1971).

In geostatistical application, a random function $Z(\mathbf{u})$ can be expressed as the sum of two parts (Dowd, 2004):

1. A deterministic part $m(\mathbf{u})$, called *drift* or *trend*, represented by a deterministic function of location (linear, quadratic or cubic).
2. A stationary random function $R(\mathbf{u})$ with a constant mean that represents the deviation from the mean $m(\mathbf{u})$, so called residuals, and can be estimated by the standard techniques of stationary methods.

If the mean $m(\mathbf{u})$ is assumed to be a constant value, then we have the basis for the geostatistical methods of overcoming the problems imposed by stationarity. A decision of stationarity of available data used for spatial modelling is necessary for all geostatistical modelling. However, as stated by Journel (1986), stationarity is a constitutive property of the random function and not an intrinsic property of the studied phenomenon and therefore a decision about stationarity is, in fact, a model itself. During the study of a geothermal reservoirs, the parameters are often considered as non-stationary, mainly in vertical direction. For example, it is well known that temperature as function of depth increases with depth (Figure 2). Matheron (1973) described the geostatistical tools for the mathematical expressions of a non-stationary phenomenon. The basic concept is Intrinsic Random Function of order k (IRF-k).

The variogram is the basic structural tool to model spatial continuity in geostatistical applications. It represents bivariate statistics, which express the variability of increments of the values z of random variables Z at points $\mathbf{u}$ separated by a vector $\mathbf{h}$. In the stationary case, the first order increments $[Z(\mathbf{u}_\alpha) - Z(\mathbf{u}_\beta)]$ filters out the constant drift. In non-stationary case, a higher order increments would be required to filter out the higher order of the drift. A specific structural analysis tool, the generalised covariance function $K(\mathbf{h})$, is defined, which filters these higher order increments instead of building a model by pasting together stationary random function and a given drift , which will generate universality condition in the kriging system (Wackernagel, 2003). The idea is to infer generalised covariance functions that filter a class of deterministic functions. The most widely used models for generalised covariance as exponential polynomials of the form:

$$K(\mathbf{h}) = b_0\delta(\mathbf{h}) + \sum_{k=0}^{K}(-1)^{k+1} b_{k+1}|\mathbf{h}|^{2k+1}. \tag{1}$$

where coefficients $b_k \geq 0$ are such that covariance $K(\mathbf{h})$ is conditionally positive definite (Dowd, 2004). Term $\delta(\mathbf{h})$ is the Dirac function, which takes into account presence or absence of the nugget effect. These conditions with corresponding covariance for order K used in practise are:

$$K=0: \quad K(\mathbf{h}) = b_0 - b_1|\mathbf{h}|,$$
$$K=1: \quad K(\mathbf{h}) = b_0 - b_1|\mathbf{h}| + b_2|\mathbf{h}|^3.$$

The polynomial covariance (1) is a nested model, built up with several structures including a nugget effect. This extended covariance is well suited for automatic fitting and inessential structures get zero weights (Wackernagel, 2003).

Geostatistical methods of estimation provide the best possible weighting for data used within estimation neighbourhood so as to produce the lowest possible error of estimation. The estimation variance, in terms of the generalised covariance, is expressed as following:

$$\sigma_o^2 = K_{oo} - 2\sum_{\alpha=1}^{n_o}\omega_\alpha K_{\alpha o} + \sum_{\alpha=1}^{n_o}\sum_{\beta=1}^{n_o}\omega_\alpha\omega_\beta K_{\alpha\beta} + \sum_{k=0}^{K}\lambda_k\left[\sum_{\alpha=1}^{n_o}\left(\omega_\alpha f_\alpha^k - f_o^k\right)\right]. \tag{2}$$

where ω_α are the weights and f^k are basic functions of the drift that depend on the degree K of the drift. For example, in three dimensional space, if we consider only z direction, the general forms of possible drift are:

$$\begin{aligned}
\text{no drift: } K=0: \ & f^0(\mathbf{u})=1 && \Rightarrow \ m(\mathbf{u})=a_0,\\
\text{linear drift: } K=1: \ & f^1(\mathbf{u})=z && \Rightarrow \ m(\mathbf{u})=a_0+a_1\cdot z,\\
\text{quadratic drift: } K=2: \ & f^2(\mathbf{u})=z+z^2 && \Rightarrow \ m(\mathbf{u})=a_0+a_1\cdot z+a_2\cdot z^2.
\end{aligned}$$

The estimation variance (2) is minimised with respect to the weights ω_α, assigned to the n_o data z_α within a search neighbourhood available for estimation of unknown value z_o, and Langrange multipliers λ_k. The minimising of the estimation variance results in an intrinsic kriging system of equation (Wackernagel, 2003):

$$\frac{\partial\sigma_o^2}{\partial\omega_\alpha}=0;\ \frac{\partial\sigma_o^2}{\partial\lambda_k}=0 \qquad \begin{cases} \sum_{\beta=1}^{n_o}\omega_\beta K_{\alpha\beta}-\sum_{k=0}^{K}\lambda_k f_\alpha^k=K_{\alpha o} & \text{for } \alpha=1,\ldots,n_o;\\ \sum_{\alpha=1}^{n_o}\omega_\alpha f_\alpha^k=f_o^k & \text{for } k=0,\ldots,K. \end{cases} \tag{3}$$

Solving the intrinsic kriging system we get a set of weight ω_α that are used in linear combination for estimating the unknown value z_o at unsampled location $\mathbf{u}_o$.

2.1 Geostatistical simulations

Geostatistics methods of estimations that are based on a simple assumption that a natural phenomenon can be considered as only one realisation of a random process. The aim of kriging is to produce the best accurate estimation of the mean value of a random variable Z at an unsampled location $\mathbf{u}_o$, $E[Z(\mathbf{u}_o)]$ in the sense of the least-square method because of minimizing the local estimation variance σ_o^2. The spatial structure of the estimated values differs from that of the actual ones (de Fouquet, 1993). The map of kriged estimates is interpreted as a set of expectations of the random variables at all locations $\mathbf{u}_o$ and tends to smooth out the local variability of the data. That means that low values are overestimated whereas high values are underestimated. The smoothing effect of kriging is a serious disadvantage when trying to reproduce the extreme values. One important fact is that the smoothing effect of kriging depends on the data location – smoothing is smaller close to the data location and conversely. The final kriged map is therefore less variable than the data.

Stochastic simulation produces a map of realisations $z_s(\mathbf{u}_o)$ of a set of random variables $Z(\mathbf{u}_o)$ at all unsampled locations $\mathbf{u}_o$. The aim of the simulations is to randomly draw several realisations of the random function that reflect the variability of the sample values (data histogram and variogram). Each simulated realisation represents a possible version of reality coherent with the data values, their statistical distribution (histogram) and a used model of variability (covariance or variogram). A simulation that does not honour the experimental data values is called non-conditional simulation (NS). There are many methods for generating a realisation of the non-conditional simulation, for example sequential methods, spectral methods, LU covariance matrix decomposition, turning bands, etc. Each method has its own advantages and disadvantages, as may be seen for example in Chilès and Delfiner (1999) or Lantuéjoul (2002). In general, non-conditional simulation is one possible realisation of a random function that has the same covariance or variogram model as the one modelled from the sample data, but it is otherwise totally unrelated to them (Chilès and Delfiner, 1999). Non-conditional simulation is conditioned by kriging. Conditioning is a process by which we can pass from a non-conditional simulation Z_{NS} to a conditional simulation Z_{CS} that match the sample points $z(\mathbf{u}_\alpha)$ of random function $Z(\mathbf{u})$. Non-conditional and conditional simulations are independent, but with the same variogram model. Conditional simulation $Z_{CS}(\mathbf{u})$ is built by adding of the kriging error $[Z(\mathbf{u}) - Z_K^*(\mathbf{u})]$ to the kriging estimation $Z_K^*(\mathbf{u})$. However, the kriging error is unknown because $Z(\mathbf{u})$ is not known. Therefore the kriging variance is replaced by non-conditional simulation of the kriging variance $[Z_{NS}(\mathbf{u}) - Z_{NS}^*(\mathbf{u})]$ where non-conditional simulation $Z_{NS}(\mathbf{u})$ is known on a simulated grid and is based on the variogram modelled from the sample data. Estimation of the non-conditional simulation $Z_{NS}^*(\mathbf{u})$ is based on kriging of the values of the non-conditional simulation at the sample locations $\mathbf{u}_\alpha$ using the same variogram model. The principle described above is shown in Figure 3.

Conditional simulation results in numerous realisations of a random function, each somewhat different from the next, depending on the amount of data available. The reason for generating multiple realisations is to enable quantitative assessment of the degree of uncertainty in the model being built. It is through these realisations that the "stochastic" characteristics become known. The degree of difference among the realisations is a measure of uncertainty. Summarising the realisations into a set of statistical metrics and displays uses the full potential of this method. There are a few important statistical summaries and summary maps to consider when evaluating a set of realisations, in particular the mean and standard deviation of the realisation and the integrated probability distribution curve. The mean and standard deviation of the realisations can be derived from post-processing and provide the ability to make and estimate of a value at an unsampled location as well as the tolerance around it (Yarus and Chambers, 2006). A set of L independent and equal probable realisations of random function from conditional simulation constitutes a **numerical model**. Simulation post-processing and ranking of the realisations from the smallest realisation to the largest one enables us to construct an inverse distribution curve for any single cell of simulated grid, a group of cells or the entire area under consideration. The curve represents a probability, or risk curve (Figure 4).

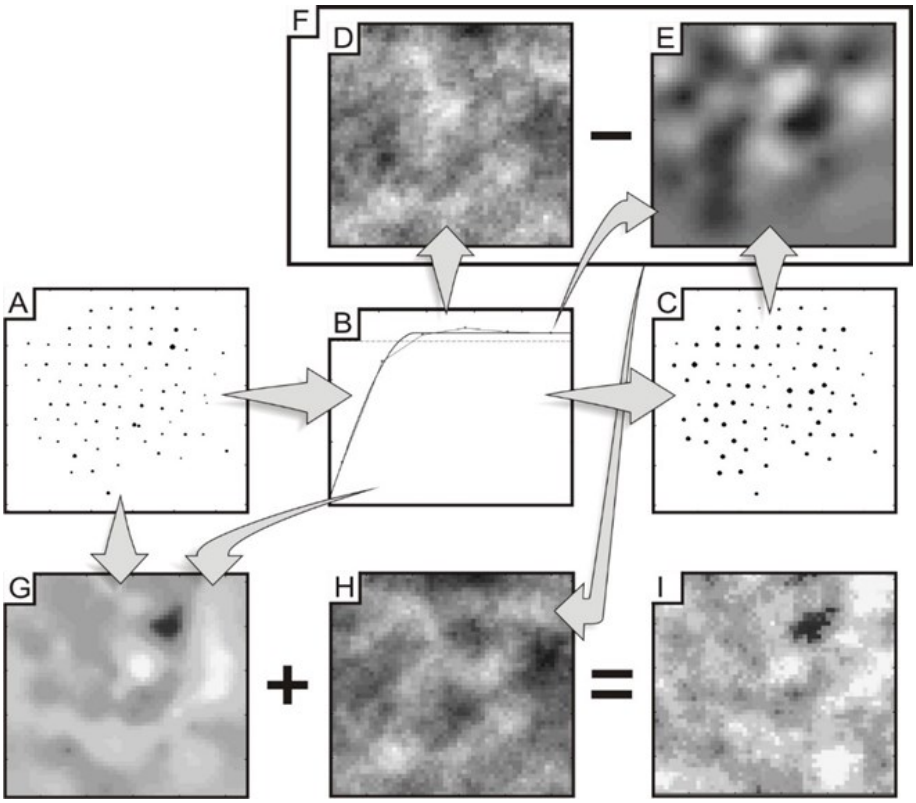

Figure 3: The principle of generating a conditional simulation as a one realisation of random function in 2D. The values at sampling locations $z(\mathbf{u}_\alpha)$ (A) are used to construct a variogram model (B). The model of variogram is used to simulate the values of the non-conditional simulation at the sample location to obtain $z_{NS}(\mathbf{u}_\alpha)$ (C) as well as on the grid nodes to get non conditional simulation $Z_{NS}(\mathbf{u})$, which represents a reality with the same variability pattern as the sample values (D) Non-conditional simulation values $z_{NS}(\mathbf{u}_\alpha)$ at the sample locations are kriged on the grid nodes using the variogram model (B) to get a smooth estimation of the non-conditional simulation (E). Difference between non-conditional simulation and kriged non-conditional simulation gives a kriging error – a natural error, which appears when a reality is estimated from the samples (F). Conditional simulation (I) is finally built up by adding the simulated kriging error (H) to the kriging estimation of a regionalized variable (G) using the sample data (A) and the variogram model (B).

2. INPUT DATA

Input data were obtained on a 3D calculation points. The points were regularly spaced in a horizontal plane with step 1 000 x 1 000 m to cover both upper (RES1) and deep reservoirs (RES2), in total 352 points for RES1 and 608 for RES2. Then, the reservoirs were vertically subdivided into four sublayers in accordance to a vertical reservoir thickness. We obtained 5 points at given position in a horizontal plane with the same X and Y coordinates. These 5 points were proportionally distributed from reservoir's top structural surface to its base. It resulted in two set of 3D calculation points with their respective **u** = (X, Y, Z) spatial coordinates; in total 1 760 points for RES1 and 3 040 calculation points for RES2.

The 3D calculation points were used to calculate a stationary geothermal model for both reservoirs. Final calculation databases include, in addition to the temperature values, different geothermal parameters. Because it is not possible to present all of the parameters, nor all results, we focused only on reservoir's temperature T [°C], exergy e [kJ.kg^{-1}] and specific exergy index $SExI$ [–] calculated within deep reservoir RES2. Table 1 shows some basic statistical characteristics of the studied variables for RES2.

Table 1: Basic statistical characteristic of the input data.

TD parameter	min	max	mean	SD *
T_RES2 [°C]	8	106	49.52	16.67
e_RES2 [kJ.kg^{-1}]	2	86	24.71	14.09
$SExI$_RES2 [-]	0.001	0.07	0.019	0.012

* SD – standard deviation

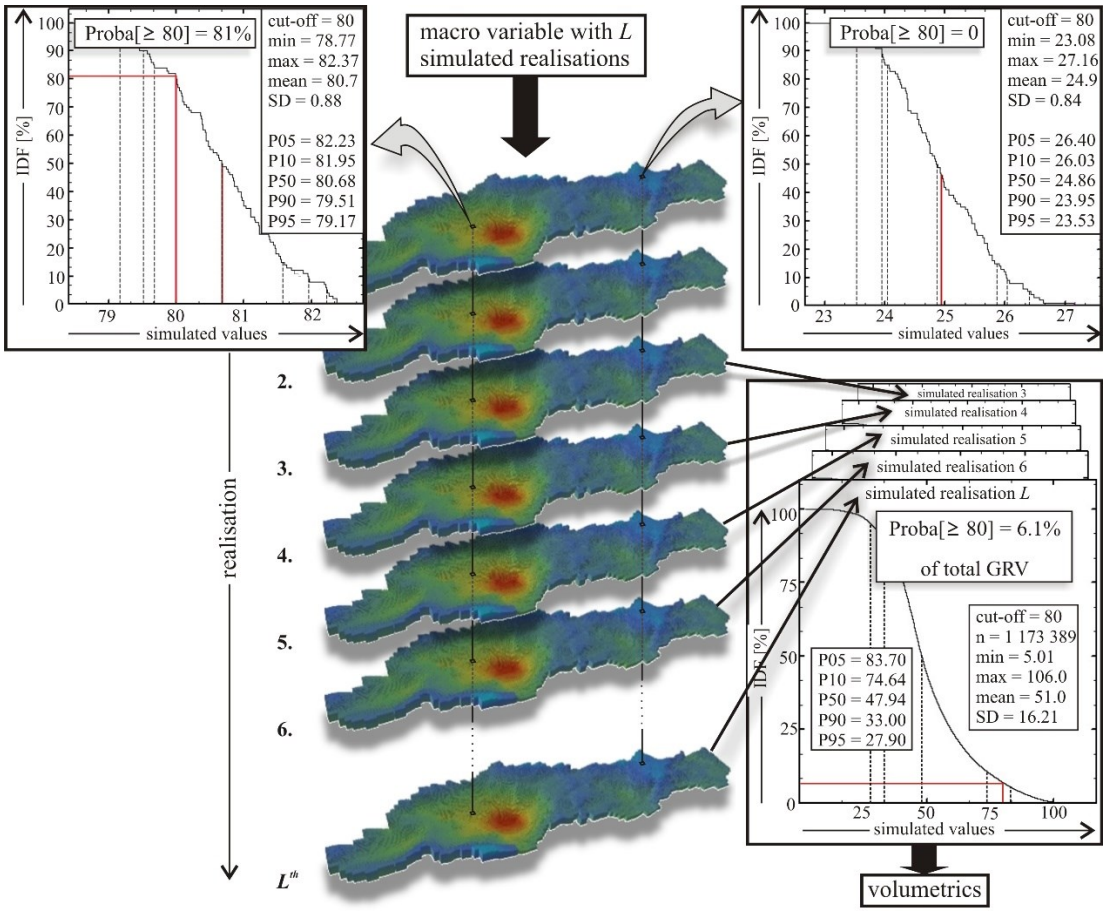

Figure 4: Principle of a numerical model post-processing.

2. RESULTS

The calculation of the stationary geothermal models, as describe previously, was perform prior to a geostatistical numerical modelling. The numerical models were created on 3D block models with resolution 100 x 100 x 25 m (total gross rock volume "GRV" equals to 250 000 m^3). Models' resolution is in accordance with provided global geological model of Liptov basin (see Figure 1). It gives 773 253 blocks for RES1 and 1 173 389 blocks for RES2 (GRV 193 313 and 293 347 Mm^3 respectively).

The ISATIS software package by Geovariances was applied to all steps of geostatistical modelling from automatic fitting both, drift and generalised covariance, to the stochastic simulations to create the numerical models of studied TD parameters, their post-processing and 3D visual inspections. We chose this particular approach of the automatic non-stationary modelling due to the fact that the global trend modelling was insufficient to filter out the trend from data in the vertical direction to obtain the stationary residuals.

The Turning Band (TB) algorithm was selected for simulation of the studied variables. The TB method development for simulations is due to Matheron (1973). It was the earliest algorithm for simulation of autocorrelated random processes in two or three dimensions (Deutch and Journel, 1998). The method consists in adding up a large number of independent simulations defined on lines scanning the 3D space. The principle consists in producing a non-conditional simulation of a random function on *N* lines independently with a given covariance model. That reflects the input histogram and covariance but does not honour the input data. Independent one-dimensional realisations are first simulated along lines radiating from central points. Then, each point or block in 3D space is orthogonally projected into every *N* lines uniformly spread out in the space and the simulated values nearest to the projected block are averaged. The non-conditional simulation is then conditioned by kriging, which is used to interpolate the experimental error between data and non-conditional simulated values at the data points by kriging algorithm. The TB algorithm is suitable for all covariance models, does not assume Gaussian type model, which is not compatible with non-stationarity assumption (Chilès and Delfiner, 1999), and it is great compromise between the output qualities and computing time.

Using simulation post-processing of 100 simulated realisations, the basic statistical characteristics for each reservoir were calculate to obtain a set of required realisation models, namely minimal realisation, maximal realisation, mean and the respective standard deviation. The derived realisation served for studying the spatial distribution of temperature and TD parameters of the numerical models on a screen.

The basic statistical characteristics of the outputs are given in Table 2. The simulated values for temperature gets values from 1.04 to 108.76 with the mean value equal to 50.98 °C. Comparing to the statistics in Table 1, we observe underestimation of the minimum of input data and overestimation of the maximum. The spreading of the experimental range of the input data is a result of using the non-stationary model, which is able to extrapolate the data range (Goovaerts, 1997). The same situation occurs for simulation of exergy data with minimal simulated value equal to 0.18, maximum 89.68 and mean value 25.76 kJ.kg^{-1}. The 100 realisations for specific exergy index differ very slightly, mainly in the maximums, since the input values are very low with a negligible variance.

Table 2: Basic statistical characteristics of statistical maps based on numerical models of TD parameters.

TD parameter	outputs	minimum	maximum	mean	SD
*T*_RES2 [°C]	minimal realisation	1.04	105.39	50.93	16.16
	maximal realisation	7.06	108.76	51.01	16.25
	mean realisation	5.11	106.34	50.98	16.20
	SD realisation	0.22	2.01	0.85	0.15
*e*_RES2 [kJ.kg^{-1}]	minimal realisation	0.18	84.75	25.73	13.91
	maximal realisation	1.47	89.68	25.79	14.03
	mean realisation	1.01	86.13	25.76	13.96
	SD realisation	0.22	0.79	0.01	0.02
*SExI*_RES2 [-]	minimal realisation	0.001	0.069	0.0196	0.0117
	maximal realisation	0.001	0.073	0.0197	0.0118
	mean realisation	0.001	0.070	0.0197	0.0117
	SD realisation	0	0.001	0	0

Next step in numerical models processing consisted in deriving the statistical and probability models for a set of cut-off values. As a matter of fact, the simulation post-processing consists in splitting a given number of simulated values into two parts – above and below a cut-off. This splitting is perform per *L* realisation for volumetrics purposes, as well as in a "vertical" direction for *L* simulated values for each block.

Table 3 lists used cut-off values for studied TD parameters. The value in grey indicates that this condition was not reached and given cut-off is irrelevant to our work.

Table 3: Cut-off values used for numerical models' post-processing.

TD parameter	cut-off 1	cut-off 2	cut-off 3
*T*_RES2 [°C]	≥ 40	≥ 60	≥ 80
*e*_RES2 [kJ.kg^{-1}]	≥ 30	≥ 50	≥ 70
*SExI*_RES2 [-]	≥ 0.005	≥ 0.05	≥ 0.2

The final statistical characteristics of the individual TD parameters above the given cut-off are summarized in Table 4. The minimal values are not listed in the table since they correspond to the respective cut-off values. Thus, the simulated values ranging from cut-off to their maximum. The mean values must be higher than cut-off value, what is fully true for our results. Notice the column "number of blocks above cut-off", which is useful information, particularly for GRV calculation above a given cut-off as a given number divided by total number of blocks times total GRV. Unfortunately, the GRV above cut-off calculated on the basis of mean values is valid only "on average". The reason is that at a given block there might be only (at least) one simulated value above a cut-off value out of all *L* simulations at the block (see Figure 4). That indicates a low probability to exceed the cut-off value at the block. Therefore, more important than mean simulation values is to answer the question what is the probability to exceed a given cut-off?

The probability of each block exceeding the particular cut-off is determined as a relative frequency of a number of simulated values above cut-off divided by total 100 simulated values so every block gets a value ranging from 0 to 1. Table 5 gives estimations of GRV above the cut-off for studied TD parameters, based on proportions of the RES2 reservoir that satisfy the cut-off conditions. There are also listed the average probabilities to meet the given cut-offs.

Table 4: Basic statistical characteristics of simulated values above a given cut-off.

TD parameter	cut-off	number of blocks above cut-off	outputs	maximum	mean	SD
*T*_RES2 [°C]	≥ 40	965 362	minimal realisation	104.53	53.53	13.89
			maximal realisation	108.76	57.52	14.17
			mean realisation	105.69	55.48	14.06
			SD realisation	1.89	0.80	0.20
	≥ 60	320 970	minimal realisation	104.53	70.62	10.61
			maximal realisation	108.76	74.36	11.15
			mean realisation	105.69	72.44	10.92
			SD realisation	1.51	0.76	0.23
	≥ 80	94 120	minimal realisation	104.53	85.52	5.61
			maximal realisation	108.76	89.12	6.33
			mean realisation	105.69	87.25	6.00
			SD realisation	1.21	0.74	0.24
*e*_RES2 [kJ.kg^{-1}]	≥ 30	359 358	minimal realisation	83.51	40.97	11.71
			maximal realisation	89.68	44.88	12.73
			mean realisation	85.18	42.86	12.25
			SD realisation	1.59	0.79	0.27
	≥ 50	106 266	minimal realisation	83.515	57.258	7.398
			maximal realisation	89.675	61.734	8.468
			mean realisation	85.184	59.402	7.961
			SD realisation	1.588	0.911	0.306
	≥ 70	20 458	minimal realisation	83.515	71.403	2.265
			maximal realisation	89.675	75.203	3.875
			mean realisation	85.184	73.053	3.035
			SD realisation	1.588	0.822	0.397
*SExI*_RES2 [-]	≥ 0.005	1 147 469	minimal realisation	0.0681	0.0187	0.0112
			maximal realisation	0.0733	0.0215	0.0119
			mean realisation	0.0695	0.0201	0.0115
			SD realisation	0.0013	0.0006	0.0002
	≥ 0.05	45 937	minimal realisation	0.0681	0.053	0.0036
			maximal realisation	0.0733	0.0567	0.0047
			mean realisation	0.0695	0.0548	0.0042
			SD realisation	0.0013	0.0008	0.0003

Table 5: Estimation of GRV for a given cut-off and mean probability of occurrence above the cut-off.

TD parameter	cut-off	GRV [Mm^3] (proportion of the RES2 in %)	mean probability above cut-off
*T*_RES2 [°C]	≥ 40	241 341 (82)	0.77
	≥ 60	80 243 (27)	0.24
	≥ 80	23 530 (8)	0.07
*e*_RES2 [kJ.kg^{-1}]	≥ 30	89 840 (31)	0.27
	≥ 50	26 567 (9)	0.08
	≥ 70	5 115 (1.7)	0.01
*SExI*_RES2 [-]	≥ 0.005	289 867(98)	0.96
	≥ 0.05	11 484(4)	0.03

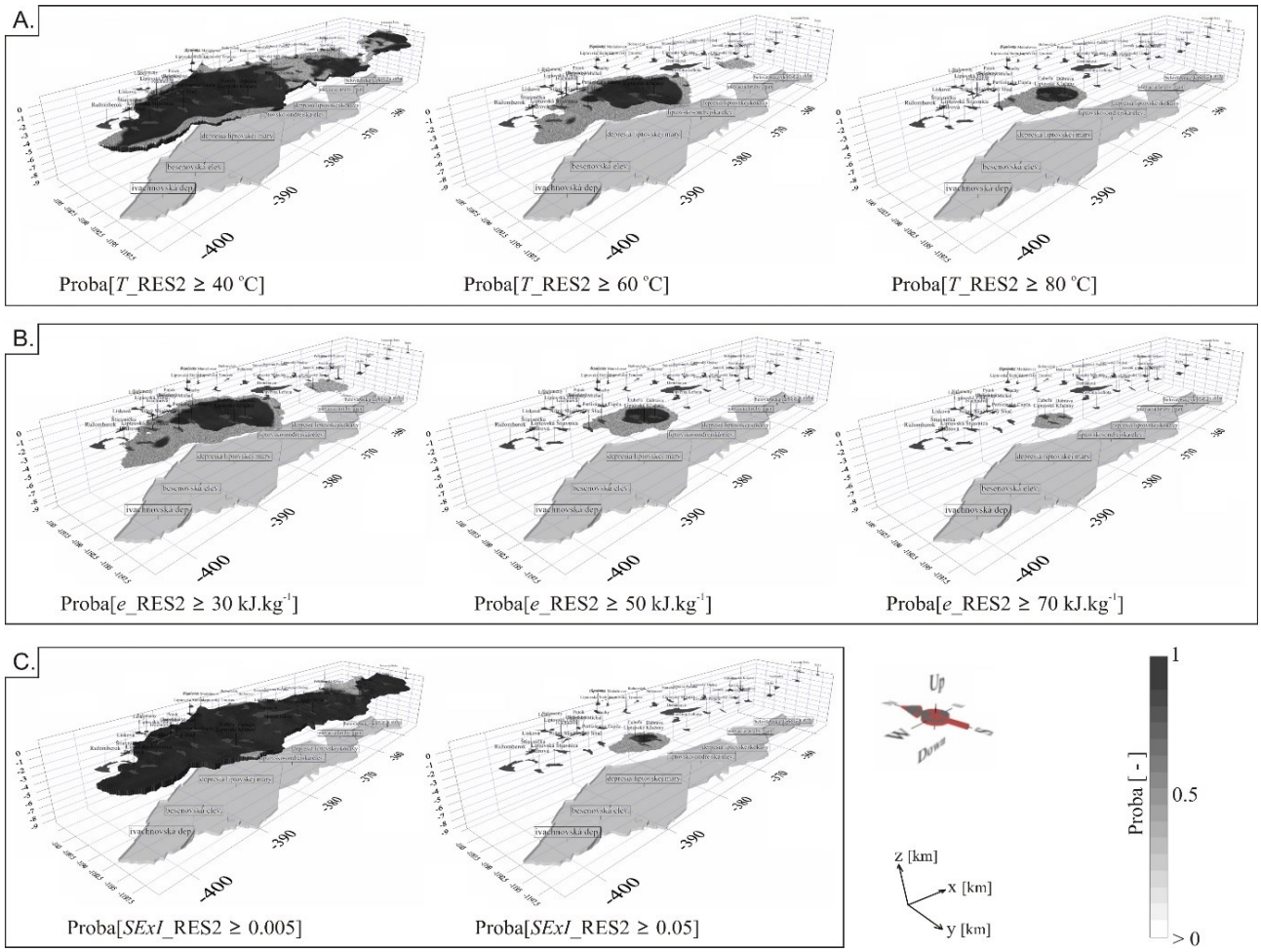

Figure 5: Spatial distributions of the estimated probabilities to exceed the cut-off values.

The results of the spatial distributions for probability estimations of studied TD parameters for different cut-offs are shown in Figure 5. The figure shows a clear relationship between the geothermal field and selected cut-offs. It can be seen that with increasing cut-off values the geothermal field volume decreases and its total volume is reduced to the area of the Liptovská Mara structure. Despite the fact that zero probabilities were excluded from the models, there are still very small probability values that are not used in decision-making process or reservoir classification. We also can see that the highest probabilities are concentrate towards to the deepest part of the RES2.

The better way than time consuming inspection of a 3D model on a screen, or reporting many 3D pictures, is a presentation of the results in form of volumetric risk curves (see Figure 4). Since a numerical model includes L simulated realisation, it is possible to calculate the volume above a given cut-off for each of them. The L volumes can by statistically processed in form of inverse distribution curve to see whit what probability we can expect a required volume or what volume we can expect for a given probability.

The results presented so far regards to the individual post-processing of the TD parameters and their respective cut-offs. In practice, the multi-conditions are applied in decision-making process. Turning now to the multi-condition case, we select the on suitable for ABCHP installation as compiled by Fričovský et al. (2024). The multi-condition account for three cut-off intervals: from 85 to 125 °C for temperature "T", from 40 to 100 kJ.kg^{-1} for exergy "e", and from 0.05 to 0.1 for exergy index "*SExI*". Note that the maximal values were not met in any case, thus multi-condition was reduced to the three following cut-offs: $T \geq 85$ °C, $e \geq 40$ kJ.kg^{-1}, and $SExI \geq 0.05$.

The number of block with simulated values above the multi-condition is 45 937, with GRV 11 484 Mm^3. This volume corresponds with less than 4 % of total GRV. Basic statistics of the simulated values fulfilling the multi-condition are given in Table 7, where we can see that the minimal values for temperature and exergy are higher than cut-off values. That means the GRV for individual cut-offs is bigger than in case of the multi-condition and the spatial distributions of these two parameters spread in subareas where the *SExI* values are lower than cut-off. We can assume that the critical parameter can be exergy index *SExI*. It can be also observed that the maximal simulated value for *SExI* is lower compare to the maximum given in Table 4. This discrepancy is due to the fact that there are no temperature nor exergy values above multi-conditions for maximal *SExI* value.

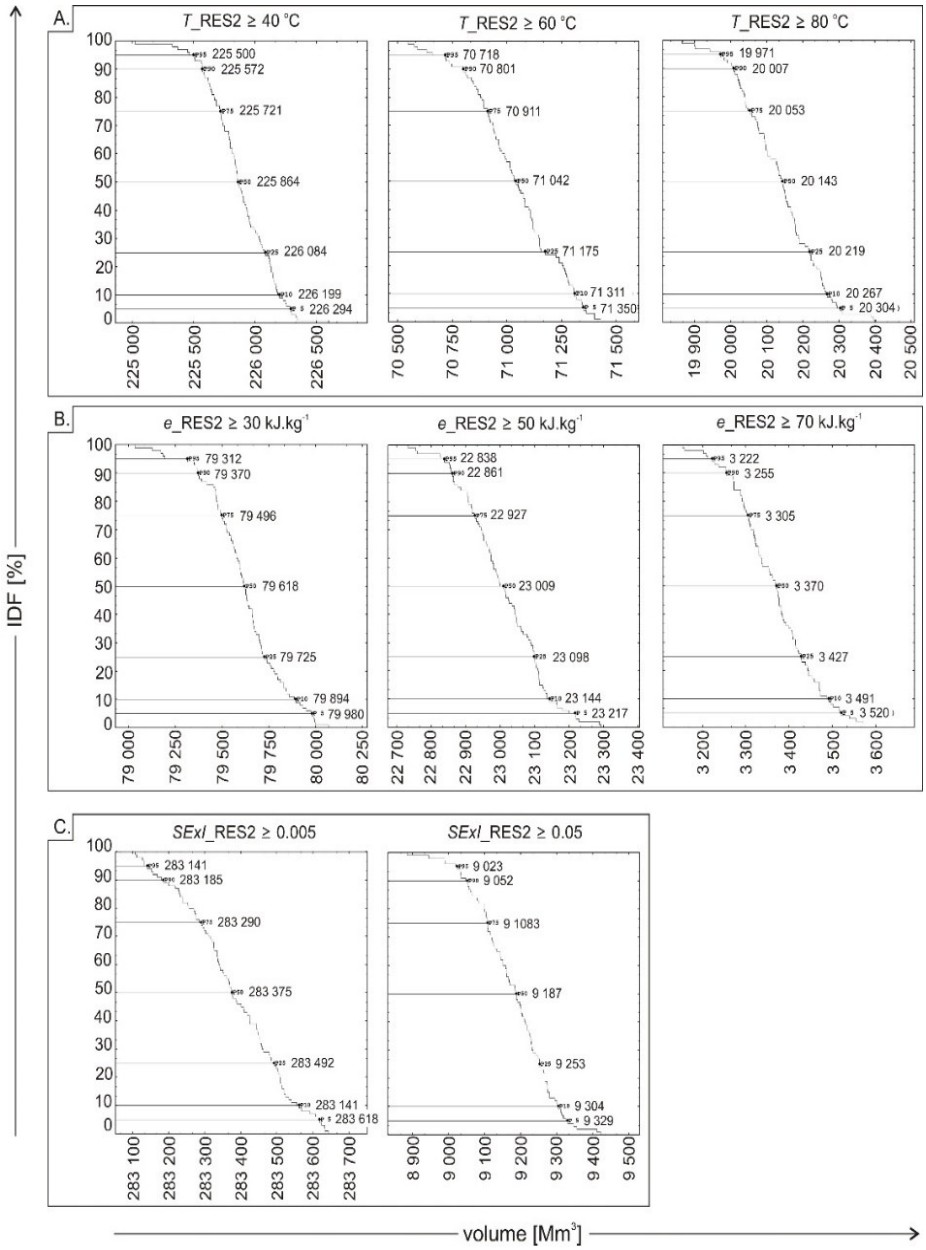

Figure 6: Volumetric risk curves above given cut-off for studied TD parameters.

Probability of the investigated multi-condition varies from 0.01.to 1 (excluding zero probabilities), with mean value equal to 0.8 and standard deviation 0.34. We can see that there are still very small probabilities. Table 7 gives basic statistical characteristics of individual probabilities of studied TD parameters based on applying the multi-condition. From the table we can note that the exergy always gets probability equal to 1 within the multi-condition. Temperature gets probability values from 0.25 to 1, but with mean equal to 0.995, which is very close to 1. Standard deviation is very small, only 0.027, which indicates that lower probability values are some individual outliers or even extreme values. The statistical characteristics of probability of occurrence *SExI* above 0.05 within the multi-condition perfectly fit the global statistics given above. That finding points to the fact, and we can conclude, that *SExI* is the most uncertain variable for evaluation a hypothetical project of the ABCHP installation.

Final spatial distributions of probabilities of occurrence studied TD parameters based on the multi-condition are shown in Figure 7, where we can observe even distributed high probabilities for temperature and exergy. The probabilities for *SExI* decrease from the deepest part of the RES2 with decreasing depth what corresponds with non-stationary assumption of TD parameters.

Table 6: Basic statistical characteristics of simulated values above multi-condition.

TD parameter	cut-off	min	max	mean	SD *
*T*_RES2 [°C]	≥ 85	85.57	105.69	92.43	4.21
*e*_RES2 [kJ.kg^{-1}]	≥ 40	57.26	85.18	67.16	5.49
*SExI*_RES2 [-]	≥ 0.05	0.05	0.07	0.055	0.004

Table 7: Basic statistical characteristics of probabilities to exceed multi-condition.

TD parameter	cut-off	min	max	mean	SD *
*T*_RES2	≥ 85	0.25	1	0.995	0.027
*e*_RES2	≥ 40	1	1	1	0
*SExI*_RES2	≥ 0.05	0.1	1	0.8	0.34

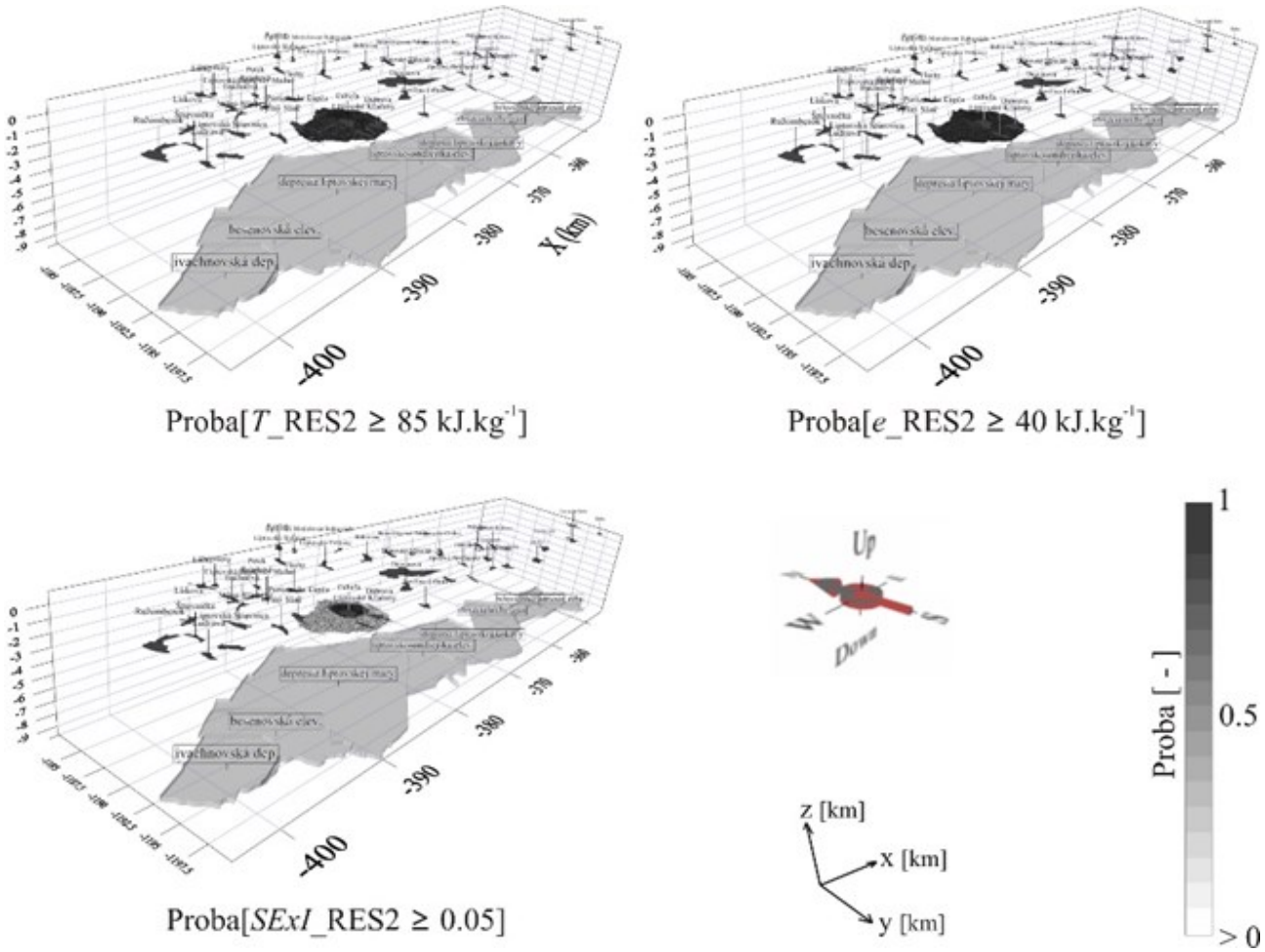

Figure 7: Spatial distribution of probabilities of occurrence the studied TD parameters above multi-condition.

3. CONCLUSION

Presented paper deals with a practical approach of geostatistical modelling for thermodynamical parameters based on calculated stationary geothermal model. Geostatistical simulations and their potential processing were presented as an alternative to the traditional way of describing of the spatial heterogeneity of geothermal areas, based on strictly data driven approach without including inherent features of a natural phenomenon such as anisotropy or non-stationarity. In our work, 3D stochastic models of the spatial distribution have been developed to describe the selected thermodynamical parameters of the deep geothermal reservoir RES2 in the Liptov basin in Slovakia.

Unlike a conventional evaluation of the geothermal potential using only temperature, this study focused on describing the reservoir under an exergy concept. The presented study quantifies, except temperature, also reservoir exergy and index of specific exergy. We have showed that non-stationarity, which is the most frequent in the geothermal reservoir's practice, has to be taken into account for prediction and simulation purposes. The simulated numerical models were processed for different cut-off, representing conditions for assessment or evaluation of the reservoir. We also established relation among the cut-offs by their combination to create multi-condition to process the numerical models to investigate the most uncertain parameter.

Our work leads us to conclude that geostatistical modelling has proved to be extremely useful for a better understanding of the reservoir's parameters that are required to provide information about the most efficient way to use geothermal energy resources, based on a balance between the purpose of a future use and the reservoir's parameters from the point of view of thermodynamic quality and reservoir potential. This pioneering study in Slovakia indicates that geostatistical tool, methods a workflows are essential to a better understanding and decreasing an uncertainty in the reservoir characterisation. Geostatistical modelling is generally assumed to be hard and difficult to apply. The presented workflows may be a time consuming but main difficulty with applying the geostatistics in the geothermal field characterisation lies in lack of knowledge.

REFERENCES

Arriaga, M.C.S. and Samaniego, F.V.: Intrinsic random functions of high order and their application to the modelling of non-stationary geothermal parameters. 23rd Workshop on Geothermal Reservoir Engineering, Stanford Univesity. (1998)

Bond C.E., Gibbs A.D., Shipton Z.K., Jones S. What Do You Think This is? "Conceptual Uncertainty*" Geoscience Interpretation*. GSA Today, v. 17, n. 11. (2007)

Chilès, J. and Delfiner, P.: *Geostatistics: Modelling Spatial Uncertainty*. John Wiley and Sons, Inc. New York. (1999) ISBN 0-471-08315-1.

de Fouquet, C.: Reminders on the conditioning kriging. In: *Geostatistical simulations pp 131–145.* Edited by Armstrong M, Dowd, P., A. Kluwer Academic, Dordrecht, (1993).

Deutsch, C., V. and Journel, A., G.: *GSLIB Geostatistical Software Library*. 2nd edition. Oxford University Press Inc. New York. (1998) ISBN 0-19-510015-8.

Deutsch, C.V.: *Geostatistical Reservoir Modeling*. Oxford University Press, Inc. New York. (2002) ISBN 0-19-513806-6.

Dowd, P.A.: *MINE5260 Non-Stationarity*. MSc. in Mineral Resources and Environmental Geostatistics. University of Leeds, U.K. (2004).

Fričovský, B., Vizi, L., Fordinál, K., Surový, M., Marcin, D.: *A reviewed hydrogeothermal evaluation of the Ďurkov depression hydrogeothermal structure: insights from probabilitstic assessment and sustainable production optimization*. In: Proceedings 44rd Workshop on Geothermal Reservoir Engineering, Stanford University, (2019).

Fričovský, B., Vizi, L., Marcin, D., Fordinál, K., Benková, K., Bottlík, F., Bahnová, N., Michalko, J., Černák, R. and Zlocha, M.: *Analysis of geothermal potential for sustainable use and utilization of geothermal resources in Slovakia – Part I*. Manuscript, Final Report, Geofond Bratislava, Slovakia. (2024) [in Slovak, English summary].

Goovaerts, P.: *Geostatistics for Natural Resources Evaluation*. Oxford University Press, Inc. 1997. London. (1997) ISBN 0-19-511538-4.

Journel, A., G.: Geostatistics: Model and Tools for the Earth Sciences. *Mathematical Geology, Vol. 18, No. 1, pp 110 – 130*. (1986)

Lantuéjoul, Ch.: *Geostatistical Simulations. Models and Algorithms*. Springer-Verlag Print, Berlin. (2002) ISBN 3-540-42202-1.

Matheron, G.: Principles of Geostatistics. *Economical Geology pp. 1246–1266*. Vol. 58. (1963)

Matheron, G.: *The theory of regionalized variables and its application.* Les Cahiers du Centre de Morphologie Mathématique. École Nationale Supérieure des Mines Paris. Fontainebleau, Paris, France. (1971)

Matheron, G.: The intrinsic random function and their applications. *Adv. Appl. Prob. Vol 5, No 3, pp. 439 – 468*. (1973)

Remšík, A., Fendek, M., Mello, J., Král., M., Bodiš, D., Michalko, J., Maďar, D., Vika, K., 1998: *Liptov basin – regional hydrothermal assessmente.* Manuscript, Final Report, Geofond Bratislava, Slovakia. (2024) [in Slovak].

Yarus, J.M and RL Chambers, R.L.: Practical geostatistics-an armchair overview for petroleum reservoir engineers. *Journal of Petroleum Technology.*, v. 58, n. 11. (2006)

Vandrová, G, Štefanka, P. Červenaj J.: *Revision of exploitation conditions for ZGL-1 and FBe-1 Bešeňová wells*. Manuscript, Final Report, Geofond Bratislava, Slovakia. (2009) [in Slovak].

Vizi, L., Fričovský, B., Fordinál, K.: Hydrothermal structures of Liptov basin — thermodynamic analysis and characteristics Manuscript, Final Report, Geofond Bratislava, Slovakia. (20025) [in Slovak].

Wackernagel, H.: *Multivariate Geostatistics*. 3rd edition. Springer-Verlag Print, Berlin. (2003) ISBN 3-540-44142-5.